Sphingolipid-mediated restoration of Mitf expression and repigmentation in vivo in a mouse model of hair graying

Bidisha Saha[1], Suman Kumar Singh[2], Shampa Mallick[3], Rabindranath Bera[4], Pijush K. Datta[5], Mriganka Mandal[1], Syamal Roy[1] and Ranjan Bhadra[1,6]

1 Infectious Diseases and Immunology Division, Indian Institute of Chemical Biology, Jadavpur, Kolkata, India **2** Centre for Skin Sciences, School of Life Sciences, University of Bradford, Bradford, West Yorkshire, UK **3** Structural Biology and Bioinformatics Division, Indian Institute of Chemical Biology, Jadavpur, Kolkata, India **4** Liver Research Unit, Chang Gung Memmorial Hospital, Kwe-Shan, Taoyuan, Taiwan **5** Department of Dermatology & STD, Medical College, Kolkata, India **6** VJRC R&D Centre, Vijoygarh Jyotish Roy College, Kolkata, India

CORRESPONDENCE Ranjan Bhadra, e-mail: rbhadra@iicb.res.in; ranjanbhdra@yahoo.com

KEYWORDS placental sphingolipid/p38 MAPK/CREB/Mitf/MKK3/6/MAPKAPK2/immunohistochemistry

PUBLICATION DATA Received 25 June 2008, revised and accepted for publication 19 January 2009

doi: 10.1111/j.1755-148X.2009.00548.x

Summary

Recent advances in the identification and characterisation of stem cell populations has led to substantial interest in understanding the precise triggers that would operate to induce activation of quiescent stem cells. Melanocyte stem cells (MSCs) reside in the bulge region of the hair follicles and are characterised by reduced expression of the microphthalmia-associated transcription factor (Mitf) and its target genes implicated in differentiation. Vitiligo is characterised by progressive destruction of differentiated melanocytes. However, therapies using UV irradiation therapy can induce a degree of repigmentation, suggesting that MSCs may be activated. As Mitf is implicated in control of proliferation, we have explored the possibility that inducing Mitf expression via lipid-mediated activation of the p38 stress-signalling pathway may represent a re-pigmentation strategy. Here we have isolated from placental extract a C18:0 sphingolipid able to induce Mitf and tyrosinase expression via activation of the p38 stress-signalling pathway. Strikingly, in age-onset gray-haired C57BL/6J mice that exhibit decaying Mitf expression, topical application of placental sphingolipid leads to increased Mitf in follicular melanocytes and fresh dense black hair growth. The results raise the possibility that lipid-mediated activation of the p38 pathway may represent a novel approach to an effective vitiligo therapy.

Introduction

Cutaneous pigmentation plays an important role in photoprotection from solar ultraviolet radiation (Kaidbey et al., 1979; Kollias et al., 1991). In the hypopigmention disorder, vitiligo (Westerhof and d'Ischia, 2007; Spritz, 2007), melanin-producing cells, melanocytes, histologically disappear. Understanding how to achieve the recovery of melanin and functional melanocytes in vitiligo patients is a major goal. Current therapies, reviewed in Falabella and Barona (2009) are only partially effective and frequently involve the use of UV irradiation, a DNA-

Significance

Vitiligo is characterised by progressive destruction of melanocytes. Although treatment strategies involving UV irradiation can be partially effective, UV may also induce DNA damage. A more effective therapy is urgently needed. Here we have shown that topical application of a lipid fraction can lead to an effective reversal of age-associated hair graying in mice. The results suggest that lipid-mediated activation of p38 stress signalling may represent a potentially effective therapy for vitiligo.

damaging agent. The non-availability of a satisfactory adjuvant therapy to treat this disorder has led to the search for new therapeutic agents capable of inducing melanoblast and melanocyte survival, proliferation, differentiation and melanogenesis. As some degree of re-pigmentation is possible in many cases of vitiligo, it is possible that while mature, differentiated melanocytes are lost, the non-pigmented melanocyte stem cell (MSC) population may remain intact. Thus, strategies designed to activate MSCs may be effective.

Recently we reported that a sphingolipid-rich placental total lipid fraction (PTLF) derived from human placenta, a rich reservoir of important biomolecules, contained activities able to induce pigmentation (Mallick et al., 2002, 2005). We subsequently showed that a nearly purified placental sphingolipid (PSL) was active as a melanin-inducing agent with mitogenic activity at low and melanogenic activity at high concentrations (Saha et al., 2006a). PSL was isolated from a vehicle-free prototype hydroalcoholic human placental extract (Bhadra et al., 1994, 1997, 1998; Pal et al., 1995), which showed pigmentation in guinea pig and C57BL/6J mouse animal models (Pal et al., 1995, 2002). The original extract was found to contain among others, lipid constituents with at least four sphingolipids (Pal et al., 1995) and screening led to identify PSL (Saha et al., 2006a) as a highly melanogenic agent. PSL was purified from this extract through a series of chromatography steps and finally obtained as a single spot by preparative high-performance thin layer chromatography (HPTLC). The HPTLC-purified PSL showed no resemblance with other standard sphingolipids spots in thin layer chromatography (TLC) (Saha et al., 2006a). Among the standard sphingolipids or sphingolipid metabolites, that modulate pigmentation, only sphingosylphosphorylcholine (SPC) is melanogenic but soluble in water (Higuchi et al., 2003). By contrast, while PSL is also highly melanogenic, its solubility is organic solvent-specific (Saha et al., 2006a).

The molecular mechanism underlying PTLF-induced pigmentation was identified as being via activation of the p38 stress-activated signalling cascade which, via phosphorylation and activation of the cyclicAMP-response element-binding protein (CREB) leads to induction of *Mitf* transcription and subsequent activation of the *tyrosinase* gene and pigmentation (Mallick et al., 2005; Singh et al., 2005; Saha et al., 2006a,b). However, the kinases upstream and downstream of p38 required for activation of Mitf were not previously identified. Here, we further characterise the chemical structural features of PSL, its capacity to activate specific components of the p38 kinase pathway and importantly demonstrate its effectiveness in stimulating pigmentation in C57BL/6J mice having age-onset hair graying. The results suggest that the PSL-induced signalling pathway may represent a safe and satisfactory therapeutic agent for treating hypopigmentary disorder, such as, vitiligo.

Results

Characterisation of bioactive PSL

As reported earlier (Saha et al., 2006a), PSL was isolated from a hydroalcoholic human placental extract by sequential column chromatography using silicic-acid and Sephadex LH 20 column and finally by scraping the single spot from a preparative HPTLC plate after repeated HPTLC to get a homogeneous spherical single spot starting from the hydroalcoholic extract of human placenta (Bhadra et al., 1994, 1997, 1998) (Figure 1A). The purity of HPTLC-purified PSL was analyzed by high-performance liquid chromatography (HPLC) (Figure 1B). A comparative TLC analysis with melanocyte activity-modulating sphingolipid metabolites are also shown therein indicating clearly that it differs distinctly from a known melanocyte mitogenic SPC (Figure 1A). Again SPC is soluble in water while PSL is not and requires organic solvents for solubilisation. Thus, PSL is not a previously known melanocyte-modulating sphingolipid metabolite.

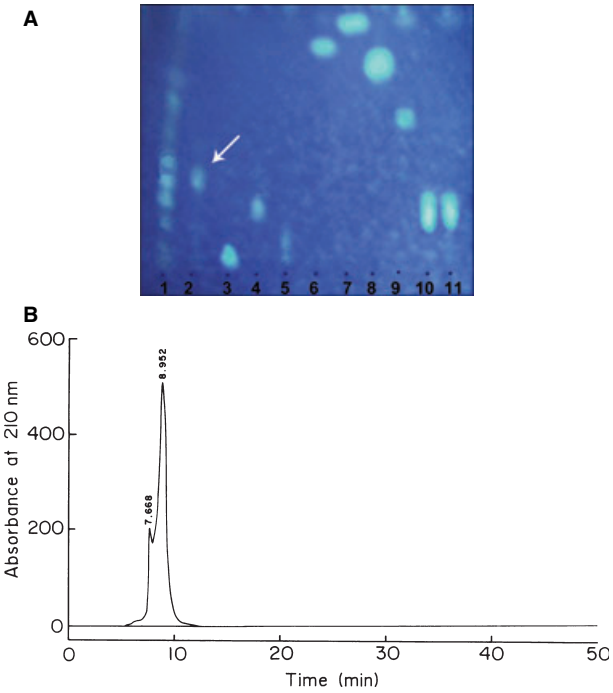

Figure 1. Thin layer chromatography (TLC) of sphingolipids and high-performance thin layer chromatography of bioactive placental sphingolipid (PSL). (A) TLC of sphingolipids was analyzed using solvent system $CHCL_3$/MeOH/H_2O (14:6:1 v/v/v) and detected by spraying the plate with primuline and made visible and photographed by illuminating under UV at 365 nm. Lane1: PTLF; lane 2: PSL; lane 3: SPC; lane 4: Sphingosine; lane 5: S1P (sphingosine-1-phosphate); lane 6: C2-Cer (C2-ceramide); lane 7: C6-Cer (C6-ceramide); lane 8: GC (glucosylceramide); lane 9: LC (lactosylceramide); lane 10: SSM (Stearoylsphingomyelin); lane 11: PSM (palmitoylsphingomyelin). Arrow in (A) denotes the PSL spot. (B) HPLC chromatogram of the HPTLC-purified PSL.

Matrix-assisted laser desorption/ionisation time-of-flight (MALDI-TOF) mass spectroscopy of the bioactive PSL showed several characteristic peaks at 301, 379,760,782 and 799 (Figure 2A). The highest molecular mass (M) of PSL generated is 759 [$(M+H)^+$ = 760, $(M+Na)^+$ = 782, $(M+K)^+$ = 799]. The 301 and 379 peaks indicated the presence of sphingosine and sphingosine phosphate in the PSL while the fatty acid analysis of PSL indicated the presence of C18:0 (methyloliate) and C16:0 (methylpalmitate) fatty acyl chains (Figure 2B).

Purified PSL induces dendrite outgrowth, tyrosinase expression and melanogenesis in human melanocytes

Although previously we reported that PSL induced melanin synthesis in B16F10 mouse melanoma cells (Saha et al., 2006a), we also wished to evaluate the effects of this bioactive sphingolipid on cell morphology and melanogenesis in human melanocytes. Distinct morphological changes and dihydroxyphenylalanine (DOPA) staining of melanocytes were observed 3–4 days after addition of stimulants as evidenced by phase contrast microscopy (Figure 3A). Most of the untreated control melanocytes exhibited bipolar dendricity with basal pigmentation levels (Figure 3A: a, b). Compared to the control cells, treatment of melanocytes with 10 μg/ml of PSL induced higher number of elongated dendrites and much higher DOPA staining reflecting increased melanin pigmentation (Figure 3A: c, d).

Tyrosinase is regulatory on the mammalian melanogenesis and the effects of PSL on its expression at the protein level in the cultured normal human melanocytes was analysed by immunofluorescence. The results (Figure 3B), revealed higher levels of tyrosinase was expressed in melanocytes after 72 h exposure to 10 μg/ml PSL compared to the basal level in untreated cells.

PSL activates the MKK3/6, p38, and MAPKAPK2 and MSK1 to induce *Mitf* promoter activity and subsequently *tyrosinase* gene expression

In our previous studies, involving sphingolipid-enriched PTLF-mediated melanogenic signal transduction in B16F10 melanoma, we reported that p38 MAPK/CREB-mediated activation of *Mitf* gene expression leads to enhanced *tyrosinase* gene expression (Singh et al.,

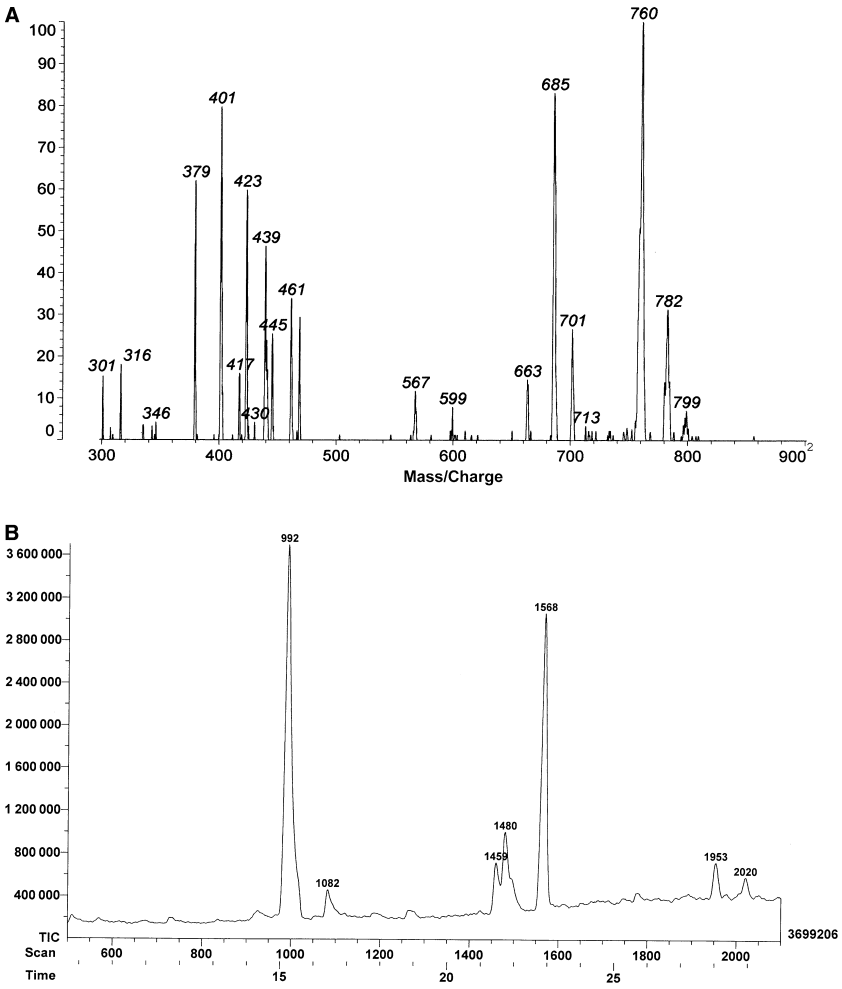

Figure 2. (A) Matrix-assisted laser desorption/ionisation time-of-flight mass spectrum of bioactive placental sphingolipid (PSL). (B) Fatty acid profile of PSL. Fatty acid methyl esters were obtained by methanolysis procedure as described in the 'Materials and methods'.

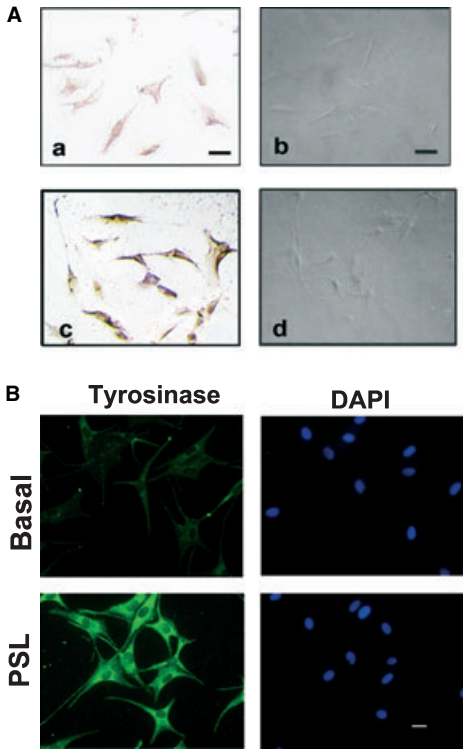

Figure 3. (A) Dendritogenesis and melanogenesis as shown by DOPA staining in normal human primary melanocytes after 4 days in the presence of PSL using the medium as described in the 'Materials and methods'. Untreated cells (a, b), 10.0 μg/ml of PSL (c, d). All cells were photographed under equal magnification by inverted phase contrast microscope. Bar represents 30 μm. (B) Immunoflurorescence labeling of human melanocytes stimulated with or without 10 μg/ml PSL for 72 h to identify tyrosinase proteins as described in the 'Materials and methods'. The tyrosinase proteins (green) (left panel) and nuclei of the cells by DAPI staining (blue) (right panel) were visualised by immunofluorescence in an inverted fluorescence microscope. All photographs are under equal magnification and bar represents 20 μm.

2005; Saha et al., 2006b). Here we determined the role of p38 MAPK-upstream kinases (MKKs) in this signalling cascade and the relevant fate of p38 MAPK substrate, CREB kinases. As, the cell cycle of primary melanocytes is very long (8–12 days) and normal healthy human skin was not easily available, the signalling studies were performed in the B16F10 mouse melanoma cell system. As shown in Figure 4A, modest MKK3 (lower band) and MKK6 (upper band) activation was detected under resting conditions and a significant increase in MKK3 phosphorylation (2.9-fold) ($P < 0.01$) was first observed within 30 min of exposure to PSL and peaked (4.1-fold) ($P < 0.001$) at about 60 min followed by a gradual decline to the basal level by 12 h. MKK6 phosphorylation was low in comparison to MKK3 phosphorylation as a very modest increase (1.8-fold) ($P < 0.01$) of MKK6 was detected after 1 h of PSL stimulation. Thus MKK3 and MKK6 activation correlates well with time-dependent phosphorylation of p38 MAPK. These data suggested that MKK3 is more preferably activated than MKK6 in B16F10 after bioactive sphingolipids stimulation.

To determine the relative contribution of MKK3 and MKK6 to PSL-stimulated p38 MAPK activation, we analyzed the phosphorylation levels of p38 MAPK and p38 MAPK kinase activity in B16F10 cells transfected with dominant negative (DN) MKK3 plasmid, pRSV-Flag-MKK3 (Ala) and DN MKK6 plasmid, pCDNA3-Flag-MKK6 (K82A) (Raingeaud et al., 1996) (a generous gift from Dr Roger Davis) separately and in combination. As shown in Figure 4B, cells transfected with DN plasmids express greater levels of immunoreactive MKK3 and MKK6 proteins compared with empty vector pcDNA3.1-transfected cells. The expression of phospho-p38 MAPK and correspondingly p38 MAP kinase activity were induced in PSL-induced empty vector transfected B16F10 cells compared with unstimulated but identically transfected cells. The DN MKK3 and DN MKK6 clones alone modestly decreased the levels of phospho p38 and p38 MAP kinase activity. However, cotransfection with both DN constructs synergistically reduced phospho-p38 MAPK compared with unstimulated empty vector-transfected B16F10 cells. These data suggested that both MKK3 and MKK6 nearly equally contribute to the PSL-stimulated p38 phosphorylation and kinase activity. However, for full activation of p38 by PSL treatment the kinase activities of both of the MKKs are essential.

We next determined the CREB-kinases responsible for PSL-induction of CREB phosphorylation in serine 133. We observed that phosphorylation of MAPKAPK2, an immediate downstream target of p38 MAPK (Stokoe et al., 1993) was evident after 30 min (2.4-fold) ($P < 0.01$) and followed a time dependent manner with maximum activation after 1 h (3.9-fold) ($P < 0.001$) and then gradually declined to the basal level by 12 h (Figure 5A, B, upper panel). The phosphorylation pattern of MAPKAPK2 was correlated well with an increase in its kinase activity (Figure 5A, B, middle panel). MAPKAPK2 was immunoprecipitated from control and PSL-treated cells and the immune complexes were assayed for phosphorylation of recombinant Hsp27 substrate, in an in vitro kinase assay with maximum activation observed at 1 h (5.57-fold) ($P < 0.01$) time point. The effect of PSL was also examined on another CREB kinase, MSK1 (Deak et al., 1998), which was activated only minimally (1.6-fold, after 1 h) ($P < 0.01$) compared to the control (Figure 5A, B, lower panel). These observations suggested that of the CREB kinases, downstream of p38 MAPK, PSL more preferentially and effectively stimulates MAPKAPK2 phosphorylation.

We also found that PSL induced a 5.3-fold ($P < 0.001$) and 4.8-fold ($P < 0.001$) (Figure 5C) increase in *Mitf* and *tyrosinase* promoter activity, respectively, compared with unstimulated controls and this PSL-responsiveness of *Mitf* promoter and subsequently *tyrosinase* promoter

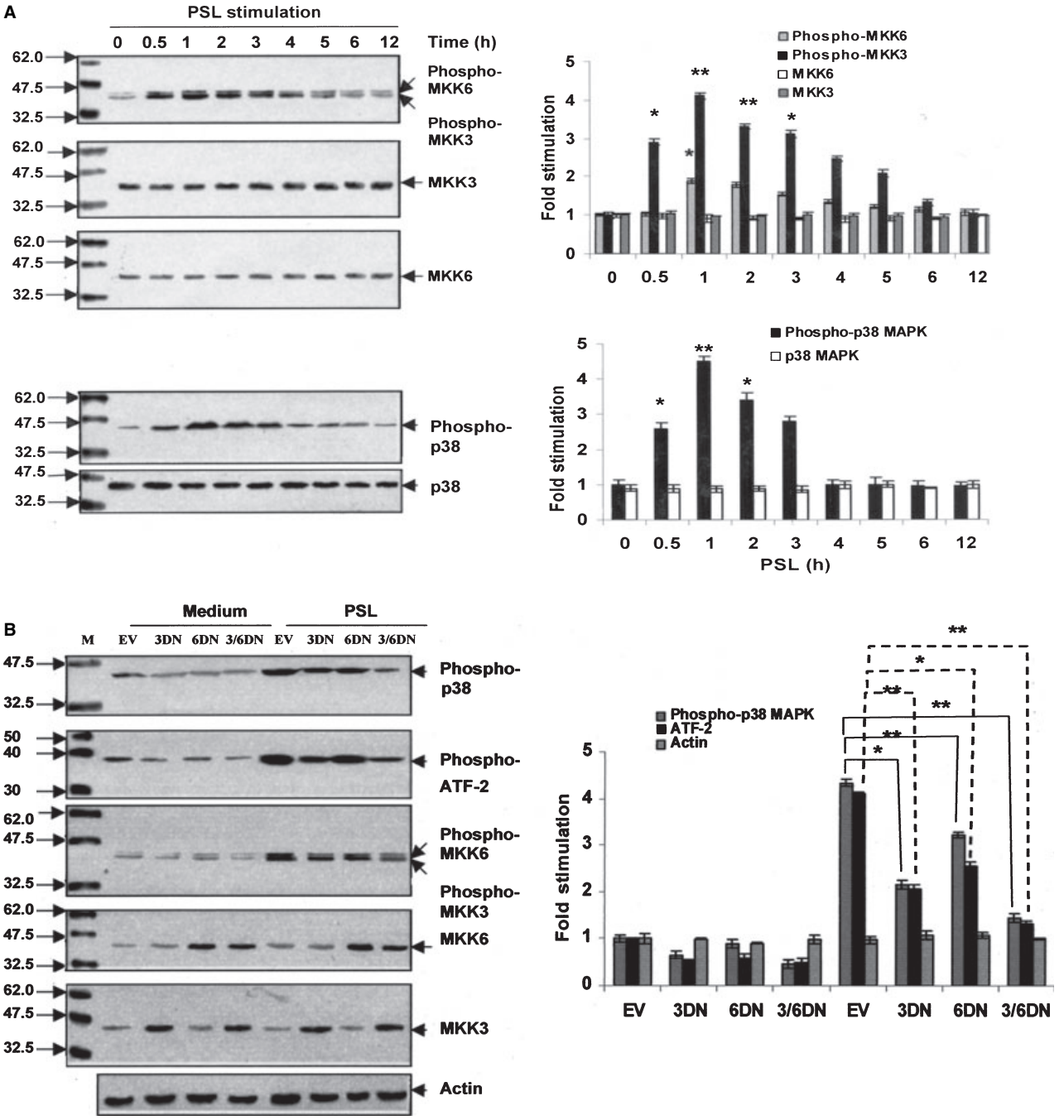

Figure 4. (A) A time course of phosphorylation of MKK3/6 (upper panel) and p38 MAPK (lower panel) in B16F10 cells in response to 10 μg/ml PSL for 0–12 h as indicated**.** MKK3/6 phosphorylation and p38 phosphorylation were analyzed by Western blot using anti-phospho MKK3/6 antibody (Ser 189/207)and anti-phospho p38 MAPK antibody (Thr 180/Tyr 182) respectively and MKK3 or MKK6 or p38 antibodies as loading control. Densitometric scanning of the band intensities of phospho-MKK3/6 (upper panel) and phospho p38 MAPK (lower panel) obtained from three separate experiments. The cumulative (control value taken as one fold in each case) data are presented as mean ± SE. *P < 0.01, **P < 0.001. (B) Effect of DN MKK3 and DN MKK6 on PSL-induced p38 MAPK phosphorylation and p38 MAP kinase activity. B16F10 cells transfected with either empty vector or DN clones as indicated. At 24 h after transfection the cells were stimulated with PSL for 1 h. Total proteins were extracted and evaluated by Western blot analysis using anti phospho-p38 MAPK, anti phospho-MKK3/6, anti MKK6 and anti MKK3 antibodies and β-actin antibody as loading control. p38 MAPK activity was determined by in vitro kinase assays using specific immunoprecipitation with anti-phospho-specific p38 MAP Kinase antibody followed by an in vitro kinase assay of its substrate, ATF-2. Densitometric scanning of the band intensities of phospho-p38 MAPK and phosphorylated ATF-2 obtained from three separate experiments. The cumulative (control value taken as one fold in each case) data are presented as mean ± SE. *P < 0.02, **P < 0.01. 3DN = DN MKK3, 6 DN = DN MKK6, 3/6 DN = cotransfection with DN MKK3 and DN MKK6.

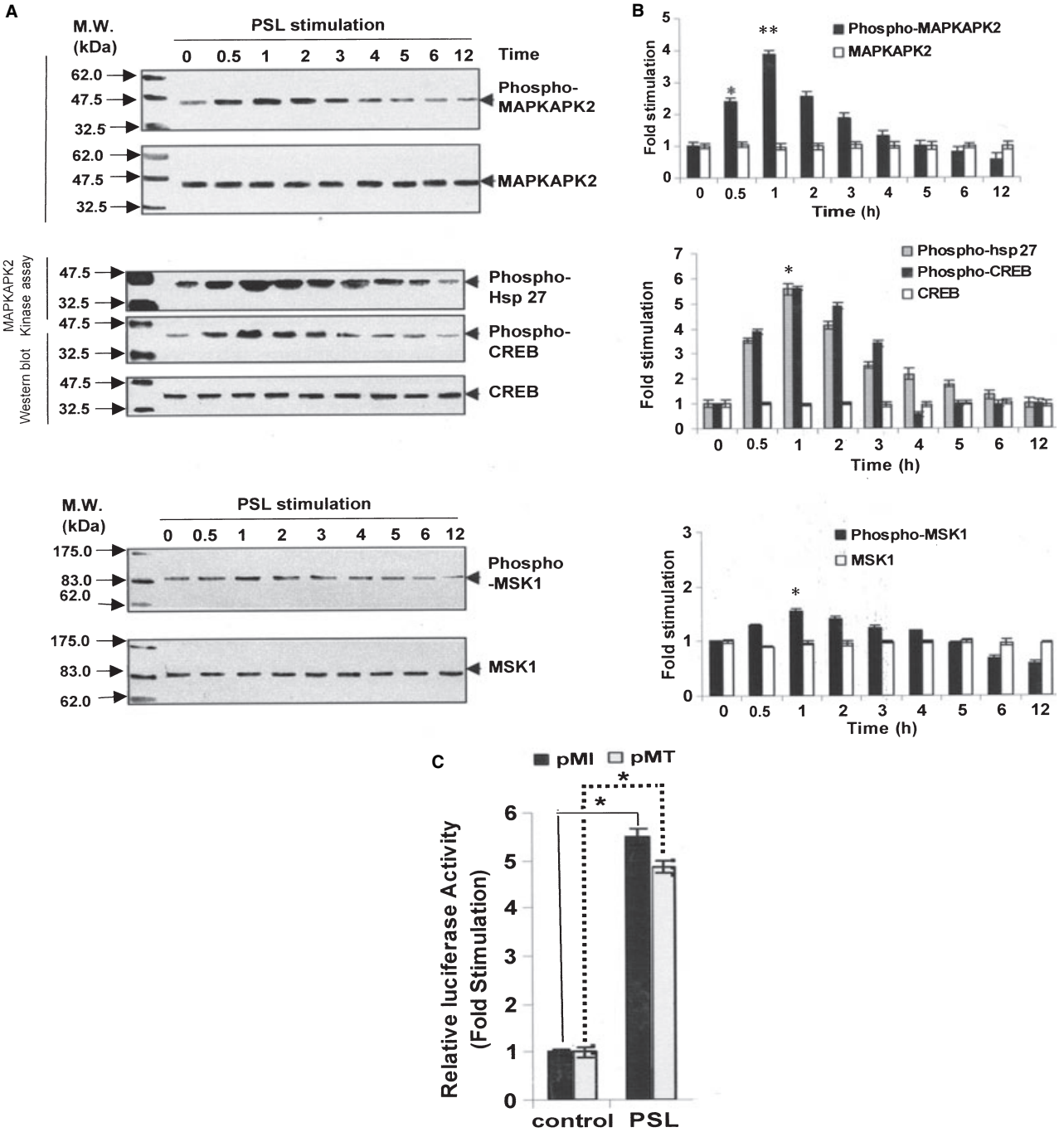

Figure 5. (A) A time course of phosphorylation of MAPKAPK2 (upper panel), MAPKAPK2 kinase activity, CREB phosphorylation (middle panel) and MSK1 phosphorylation (lower panel) in B16F10 cells in response to 10 μg/ml of PSL for 0–12 h as indicated. MAPKAPK2, CREB and MSK1 phosphorylation were analyzed by Western blot using antibody specific for Thr 222-phosphorylation of MAPKAPK2, antibody specific for Ser 133-phosphorylation of CREB and antibody specific for Ser 376-phosphorylation of MSK1; and MAPKAPK2, CREB and MSK1 antibodies as loading control. MAPKAPK2 activity was measured by a specific immunoprecipitation with anti-phospho-specific MAPKAPK2 antibody followed by an in vitro kinase assay of its substrate, hsp-27 as described in the 'Materials and methods'. (B) Densitometric scanning of the band intensities of phospho-MAPKAPK2 (upper panel), phosphorylated hsp-27 and phospho-CREB (middle panel) and phospho-MSK1 (lower panel) obtained from three separate experiments. The cumulative (control value taken as one fold in each case) data are presented as mean ± SE. *P < 0.01, **P < 0.001. (C) Effect of PSL on Mitf and tyrosinase promoter activity. *Mitf* and *tyrosinase* promoter activity was detected in B16F10 cells transfected with pMI (containing *Mitf* promoter upstream of the luciferase coding sequence) or pMT (containing a 2.2-kb pair fragment of the *tyrosinase* promoter upstream of the luciferase coding sequence as a reporter gene) along with pCMVβGal. Then cells were treated for 6 h or 12 h for pMI or pMT respectively with PSL. Luciferase activity was normalised by pCMVβ-galactosidase activity and the results were expressed as fold stimulation of luciferase activity from unstimulated control. The cumulative (control value taken as one-fold in each case) data are presented as mean ± SE. *P < 0.02.

was higher when compared with PTLF (100 μg/ml) as reported before (Saha et al., 2006b). These results agree with our earlier observations of higher protein and mRNA expression of *tyrosinase* in PSL-treated cells than that in PTLF-treated B16F10 cells (Saha et al., 2006a). Thus, it is conceivable that the purified bioactive PSL transduces melanogenic signals within cells more effectively when applied solely in purified form than in a mixture with other lipids in PTLF.

Induction of skin and hair pigmentation by PSL in age onset gray-haired C57BL/6J mice

The results presented so far indicate that in cultured cells PSL induces pigmentation via p38 signalling-mediated activation of Mitf and Tyrosinase expression. To determine the effects of PSL on pigmentation in vivo we used the C57BL/6J mouse model that exhibits age-related hair graying. After removal of gray hair of C57BL/6J mice by clipping, PSL was applied topically to the skin. Vehicle only-treated skin from the same mouse was used as a control. In contrast to vehicle (60% aqueous alcohol-) treated region which did not show any marked change in skin color from the initial pinkish appearance (Figure 6A: a), within 12 days of PSL application the skin in the PSL-treated region took on a bluish appearance (Figure 6A: b), and as the experimentation progressed the color darkened gradually. Within 25 days black hair started appearing in the PSL treated region (Figure 6A: c) similar to that found in young animals reverting telogenic phase of hair growth cycle to anagen whereas the vehicle-treated region exhibited nearly unchanged gray hairs (data not shown).

Mouse skin specimens from both the vehicle and PSL-treated sites were examined histologically under both the longitudinal (Figure 6B: a, b) and cross-sectional (Figure 6B: c, d) views after Masson–Fontana staining to compare skin organisation, melanisation and the hair follicle formation. Longitudinal view of PSL-treated skin specimen (Figure 6B: b) shows new hair follicles rooted beyond the dermis in the bulbs and embedded into the adipocyte layer unlike the vehicle-treated ones having hair bulbs within dermis (Figure 6B: a). In the cross-sectional view of the experimental specimen (Figure 6B: d), a large number of hair follicles along with corresponding melanising centers was observed compared to a few in vehicle-treated skin (Figure 6B: c).

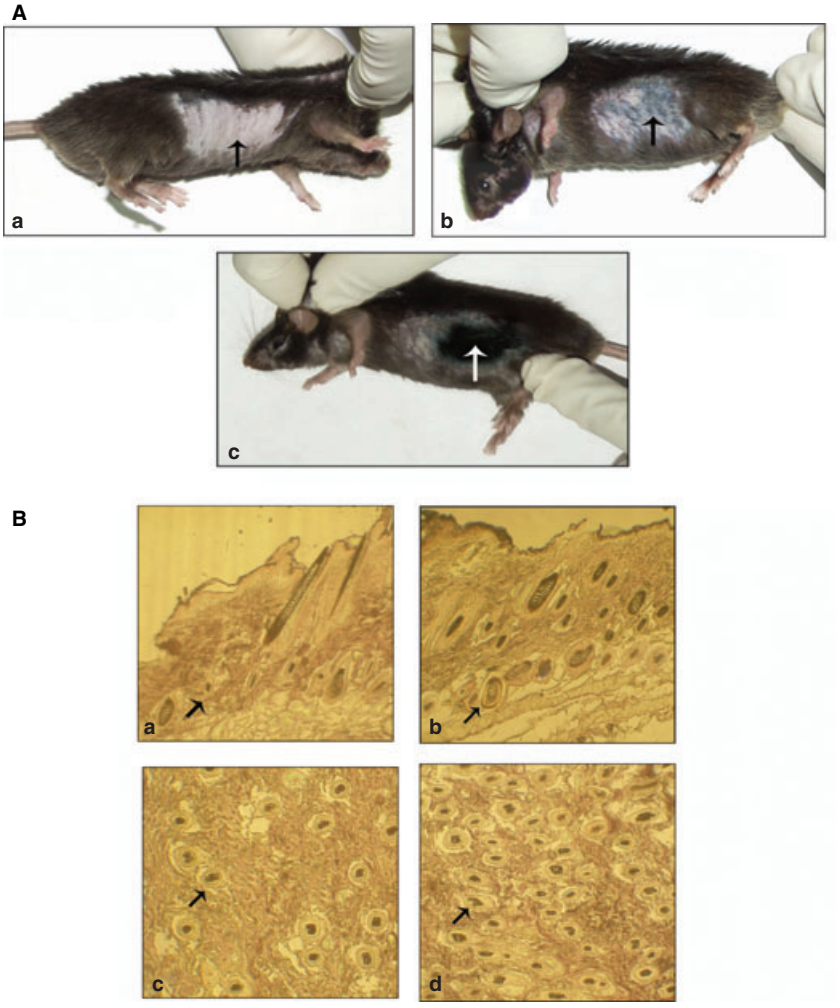

Figure 6. (A) Effect of placental sphingolipid (PSL) application on skin and hair pigmentation in C57BL/6J mice at the age-induced telogenic stage of hair growth, marked by pinkish skin and graying of hair (a) and (b). Vehicle and PSL-applied regions on the right and left sides respectively of the same mouse. Arrow in (b) denotes the PSL-treated region with the recurrence of the anagenic stage, as manifested by appearance of bluish skin. The arrow in (a) denotes control (vehicle)-treated zone with no such growth cycle reversal. (c) PSL-applied regions (arrow) on the left side of the mouse shows distinct indications of growth cycle reversal to the anagenic stage, as shown by the growth of deep black shiny hair. (B) Longitudinal (a, b) and cross-sectional (c, d) views of the skin specimens stained with Masson and Fontana stain; (a) Vehicle-treated mouse skin where the hair follicles are short, thin, few in number (arrow), and within the dermal layer, which is dense or hypotrophic as in the cross-sectional sample. (b) PSL-treated mouse skin where a hypertrophic structure and an ample number of new hair follicles can be seen (arrow) in the adipocyte layer (magnification, ×200). (c) Vehicle-treated mouse skin with a few melanising centers (arrow) in the dermal layer which is dense or hypotrophic. (d) PSL-treated mouse skin with a large number of melanising centers (arrow), (magnification, ×400).

Effect of PSL on Mitf expression of Hair follicle melanocytes-subpopulations in an age onset gray haired C57BL/6J mouse

In C57BL/6J black mice, melanocytes progressively disappear from the epidermis shortly after birth and are present only in the hair follicle (Yoshida et al., 1996). In the hair follicle, MSCs are maintained in the niche at the bulge region of the hair follicle, whereas, fully differentiated melanocytes reside in the hair bulb adjacent to the upper part of the dermal papilla (Nishimura et al., 2002; Fuchs et al., 2001). Mitf is expressed in differentiating melanoblasts and fully differentiated melanogenically active melanocytes but not in non-differentiated melanocyte stem cells (Osawa et al., 2005; Nishimura et al., 2005). Thus, Mitf may be considered as a sensitive and specific melanocyte marker for identifying the non-stem cell melanocyte populations (King et al., 1999). We used Mitf immunostaining to visualise the expression of Mitf in the hair follicle melanocytes in both vehicle and PSL-treated skin. In the hair follicles of vehicle-treated skin (Figure 7A) there were few Mitf+ cells in both the hair bulb and bulge regions representing differentiated melanocytes and undifferentiated melanoblasts, respectively. This is consistent with the characteristics of physiological hair graying with gradual loss of both undifferentiated MSCs and differentiated melanocytes from hair follicle niche and hair matrix, respectively, with aging (Nishimura et al., 2005). By contrast, numerous strongly Mitf-expressing melanocytes (higher green fluorescence) with dendritic appearance were observed in hair bulbs adjacent to the dermal papilla of PSL-induced anagenic hair follicles (Figure 7B, C and D). These were assumed to be differentiated melanocytes. A large number of Mitf+ cells were also located at the outer root sheath around the bulge region of PSL-induced anagenic hair follicle (Figure 7B, C). These are comparatively small and round in shape and most likely represented undifferentiated melanoblasts or a transit amplifying population derived from MSCs. The level of Mitf expression is therefore markedly upregulated in both the melanocytes and melanoblast subpopulations of the hair bulb and outer root sheath of PSL-treated skin specimen compared with vehicle-treated skin specimen where the intensity of staining for Mitf was significantly low.

Discussion

The results presented here provide evidence that a novel, alcohol-soluble C18:0 sphingolipid (PSL) derived from placental extract is able to stimulate melanogenesis and increase dendricity in melanocytes. The molecular mechanism underlying the PSL-mediated pigmentation was shown to be mediated via the p38 stress signalling pathway in which PSL activates both MKK6 and MKK3 which in turn leads to activation of p38 kinase and its downstream effector MAPKAPK2,

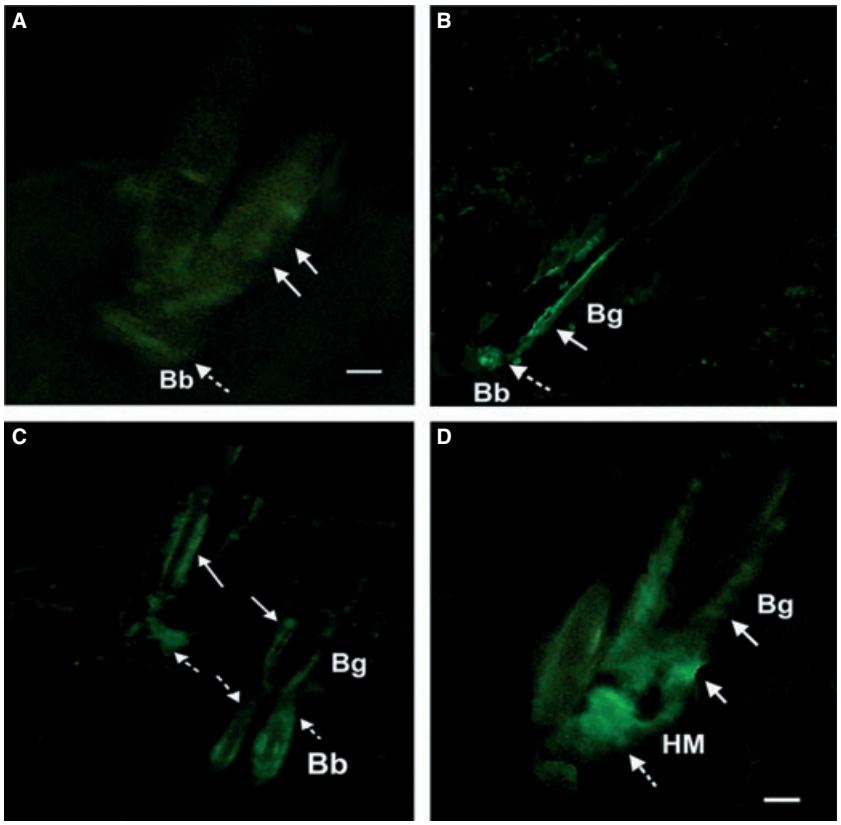

Figure 7. Immunohistochemical staining for Mitf in vehicle (control) and PSL-applied skin of C57BL/6J mouse showing distribution of Mitf+ cells (green fluorescence) in anagenic hair follicles. (A) Distribution of Mitf+ melanocytes (dashed arrow) in hair bulb (Bb) and Mitf+ melanoblasts (solid arrow) on outer rootsheath in the hair follicle of vehicle-treated skin. (B) and (C) A large number of Mitf+ melanocytes (dashed arrow) in the hair matrix around the dermal papilla and Mitf+ melanoblasts (solid arrow) on the outer root sheath in the hair bulge (Bg) of PSL-treated skin. Melanocytes are identified with dendritic morphology; melanoblasts are comparatively small and rounded in shape. (magnification, ×200; scale bar, 60 μm). (D) Magnified view of hair follicle of PSL-treated skin. Melanocytes (dashed arrow) are located in the hair matrix above the dermal papilla, (magnification, ×400; scale bar, 60 μm).

and to a lesser extent MSK1. The ability of activated MAPKAPK2 to phosphorylate and activate the transcription factor CREB leads to increased expression from the Mitf promoter and consequent activation of the Mitf target gene Tyrosinase. Our findings agree with earlier reports where CREB phosphorylation on serine 133 occurred in a p38 MAPK/MAPKAPK2-dependent manner in SK-N-MC cells (Tan et al., 1996), PC12 cells (Rouse et al., 1994) or CH31 B cell lymphoma (Swart et al., 2000) in response to fibroblast growth factor (FGF) and arsenite, nerve growth factor (NGF) or B cell Ag receptor (BCR) ligation, respectively. Thus, PSL has emerged as a highly potent pigment inducer and major active principle of PTLF through its ability to enhance Mitf expression and subsequently upregulation of tyrosinase gene substantiating Mitf as a master transcription regulator of melanocyte activity.

Vitiligo is characterised by progressive destruction of differentiated melanocytes. However, the repigmentation that can be achieved, for example by UV therapy, suggests that non-pigmented Mitf-negative MSCs are likely to remain intact. Indeed, hair follicles in vitiliginous regions are the prime reservoir of melanocyte stem cells (Fitzpatrick et al., 1983), which are, in turn, the primary source of pigment recovery. Age-induced prolonged telogen phase of hair growth cycle with the histological disappearance of follicular melanocytes in C57BL/6J black mice (Slominski and Paus, 1993) displaying gray hair is related to the depigmentation in vitiligo. Because the life and activity of a melanocyte (proliferation and differentiation) is tightly coupled with the hair growth cycle, regrowth of the pigmented hair and appearance of pigment in the skin, could be proposed synonymous with the induced growth and melanogenesis of melanocytes, concurring with repigmentation achieved in successful vitiligo therapy (Medrano and Nordlund, 1990; Slominski and Paus, 1993; Pal et al., 2002). If a prolonged telogen phase of hair growth can be converted to the anagen phase (visualized by a change in skin color with the growth of black hair) using an agent, then it is expected to be capable of inducing repigmentation in vitiligo lesions (Ortonne and Prota, 1993; Pal et al., 2002). In this respect, the ability of PSL to induce the appearance of bluish skin and the growth of fresh black hair in PSL-treated mouse skin was striking, and indicated a quick resumption of anagenic phase from prolonged telogenic phase of hair growth cycle. Intriguingly, histological examination of PSL-treated skin revealed an enhancement in the number of melanin-forming centres and an increased number of new hair follicles similar to those found by Cui et al. (1991) and Pal et al. (2002). The activity of the purified PSL reported here is most likely related to the effects of a complex mixture of peptides, amino acids and different classes of lipid in a placental extract on skin darkening in a guinea pig model (Pal et al., 1995) and hair pigmentation coupled with hair growth in C57BL/6J mice (Pal et al., 2002).

Hair graying in both mouse and humans is caused by lack of maintenance of MSCs in the niche of hair follicle which results in loss of melanogenically active progeny (melanocytes) in the hair matrix with aging (Nishimura et al., 2005). Acceleration of this process by mutation of the *Mitf* gene ($Mitf^{vit}$) implicates Mitf in the self-renewal and maintenance of MSCs (Nishimura et al., 2005). The dependence of melanocyte development on Mitf expression is obvious and the loss of viable melanoblasts or melanocytes arises due to *Mitf* mutations (Hodgkinson et al., 1993; Hughes et al., 1993). Mitf regulates melanocyte development, proliferation, survival as well as differentiation (Tachibana, 2000; McGill et al., 2002; Vance and Goding, 2004). In particular, it has been demonstrated that depletion of Mitf in melanoma cells leads to a G1-arrested stem-cell like phenotype (Carreira et al., 2006). It seems likely, therefore, that up-regulation of Mitf may represent a strategy for stimulating reserve MSCs to divide. In normal stem cells, activation of Mitf expression is likely to be controlled by Wnt signalling via β-catenin to the *Mitf* promoter (Takeda et al., 2000), as Wnt controls the generation of new hair folicles (Silva-Vargas et al., 2005). In the case of the repigmentation in the gray haired C57BL/6J achieved here, activation of Mitf expression most likely potentiates MSC proliferation, migration to hair matrix and subsequently differentiation into mature and melanogenically active melanocytes in the hair bulb as a result of PSL-mediated activation of p38, MAPKAPK2 and CREB.

The appearance of pigmented skin after PSL treatment in C57BL/6J mouse is also significant. In mice, melanocytes are generally confined to the hair follicles in the epidermis (Yoshida et al., 1996). Nishimura et al. (2002), demonstrated the epidermal repigmentation process using Dct-lacZ/+transgenic mice and showed that bulge stem cells are the source of melanocytes in the epidermis. Significantly, Mitf also regulates dendrite formation and melanoblast migration (Carreira et al., 2006; reviewed in Vance and Goding, 2004). Therefore, the appearance of blue skin and subsequently growth of anagenic black hairs after PSL application may be explained by the enhancement of Mitf expression in the bulge stem cells which then proliferate and migrate to the epidermis and the hair bulb, undergo reactivation at the next early anagen and differentiate to produce melanin pigments. The phenomenon of differentiation of the hair follicle premelanocytes into active forms and their subsequent migration to the epidermis are the key events for repigmentation in vitiligo lesions. The potential ability of the PSL to promote MSC division is of crucial importance in view of any potential therapy for vitiligo. Indeed, the pigment induction process in C57BL/6J mouse after PSL induction is reminiscent of the pigment recovery process of human vitiligo, characterised by loss of melanocytes. Based upon our results, the following model (Figure 8) for the PSL-induced

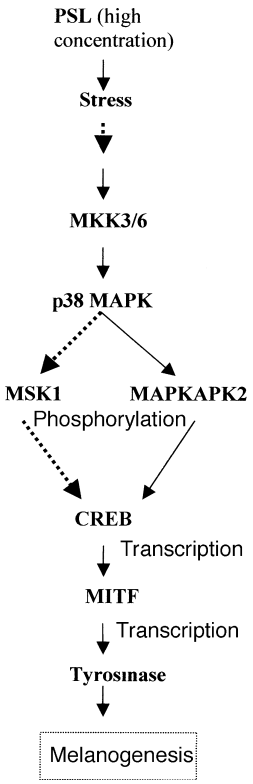

Figure 8. Proposed model for stress-signalling pathways induced by purified bioactive placental sphingolipid (PSL) leading to melanogenesis.

signalling pathways leading to melanogenesis is proposed. Thus, the detail signalling pathway induced by PSL provided the scientific basis to offer a safe and satisfactory therapeutic use of PSL for pigment recovery in depigmented skin diseases, such as, vitiligo.

Finally, while we have focused our attention here on a use for PSL in vitiligo, we are also aware that the generation of sphingolipids and activation of Mitf via the p38 signalling pathway may be an important event in the UV-mediated tanning response. Further work will be necessary to detemine the importance of lipid intermediates in UV stimulation of melanocytes.

Materials and methods

Materials

Diethyl ether, n-octanol, ethanol, HPLC grade methanol and water were purchased from E Merck India Ltd, Mumbai, India. Isopropanol, n-hexane, petroleum ether, chloroform, acetone from Spectrochem Pvt. Ltd., Mumbai, India; Silicic acid from SRL, Sisco Research laboratory, Pvt. Ltd., Mumbai, India; Primulin and iodine crystal from Sigma Chemical Co., St., Louis, MO, USA; TLC and HPTLC plate from E. Merck, Germany. Dulbecco's Modified Eagle Medium (DMEM), fetal bovine serum (FBS), penicillin, streptomycin and neomycin antibiotic, OPTI-MEM reduced serum medium and other medium supplements were obtained from Gibco BRL (Grand Island, NY, USA). Horseradish peroxidase-conjugated secondary antibodies were from Sigma Chemical Co., St Louis, MO, USA. MAPKAP Kinase2 Immunoprecipitation assay Kit (non-radioactive, no. 17–297) was purchased from, Upstate, Lake Placid, NY. p38 MAP Kinase (Nonradioactive) Assay Kit (no. 9820), Chemiluminescent Horseradish peroxidase Western blot detection system (LumiGLO Reagent and peroxide no. 7003) and primary antibodies phospho-p38 MAP Kinase (Thr180/Tyr182, no. 9211), p38 MAP Kinase (no. 9212), phospho-CREB (Ser 133, no. 9191), CREB (no. 9192), phospho-MAPKAPK2 (Thr222) (no. 3044), MAPKAPK2 (no. 3042), phospho-MSK1 (Ser 376) (no. 9591), phospho-MKK3/MKK6 (Ser189/207) (no. 9231), MKK3 (no. 9232), MKK6 (no. 9264) were purchased from Cell Signaling Technology, Inc. Beverly, MA, USA. Another primary antibodies MSK1 (no. sc-9392) and Actin (no. sc-7210) were purchased from Santa Cruz Biotechnology, Inc. Santa Cruz, CA, USA, Luciferase Assay System and β-Galactosidase Enzyme Assay System were from Promega, Madison, WI, USA.

Cell culture

Normal human melanocytes (NHMC), derived from the surgical skin specimen (provided by Prof. P. K. Dutta of Calcutta Medical College), were cultured in an in vitro system according to the modified method of Eisinger and Marko, 1982, and standardised in our laboratory. Briefly, after removal of the subcutaneous fat, small pieces of the skin specimen were prepared to treat with 0.25% trypsin, 0.05% EDTA, PSN in phosphate-buffered saline (PBS) overnight at 4°C. The epidermis was separated from the dermis by the means of forceps and the tissues were transferred to a centrifuge tube containing trypsin solution and vortexed. The resulting cell suspension was centrifuged at 500 × *g* for 10 min to pellet down the cells. The cells were resuspended in MCDB153 growth medium supplemented with 50 ng/ml of 12-O-tetradeconoyl phorbol 13-acetate, 0.1 mM isobutylmethyl xanthine, 6 ng/ml of bFGF, 5 μg/ml of insulin, 1 μg/ml of transferrin, 0.18 μg/ml of hydrocortisone, 5% FBS and PSN and plated onto 25 cm^2 culture flasks and maintained in a humidified incubator with 5% CO_2 at 37°C. Twenty-four hours later medium was replaced and thereafter changed regularly every 2 days with fresh medium. When almost 70% confluency was reached cells were passaged and used for the experiment. In experiments to evaluate the effect of PSL on melanocytes, the cells were seeded in 24 well plates at a density of 1×10^4 cells per well. The medium used in the experiment was prepared without supplementation or addition of the growth factors, TPA, BPE, IBMX and bFGF.

B16F10, a mouse melanoma procured from National Centre for Cell Science, Pune, India was cultured and maintained as before (Mallick et al., 2002). Then 1×10^6 cells/well were plated and cultured in DMEM for 24 h and the spent medium was removed with continued culturing in DMEM with 2% heat-inactivated FBS and 1% PSN antibiotic, with or without supplementation of the 10 μg/ml of PSL.

Preparation of the PTLF and PSL in brief

Placental total lipid fraction was prepared from a vehicle-free prototype human-placental extract (Bhadra et al., 1998; Pal et al., 1995) following the solvent partitioning technique (Siddiqui et al., 1998; patent) as reported previously (Mallick et al., 2002, 2005) based on a published method (Osborne, 1986). To make PSL, briefly, the residual sticky mass obtained from the placental extract by flash evaporation, was dissolved in *N*-octanol and loaded in silicic-acid column and stepwise sequentially eluted by chloroform and methanol gradient with increasing methanol concentration. The active fraction was further resolved by chromatography using, sephadex-LH20 column, and finally by preparative HPTLC. HPTLC resolved single band was scraped off and repeatedly resolved and finally run on a TLC plate with the solvent system chloroform–methanol–water (14:6:1 v/v/v). A fine single spot of the lipid was lighted up in

iodine, premulin and benzidine spray. PSL was found with high pigmenting activity in B16F10 melanoma cells in vitro.

High-performance liquid chromatography analysis

High-performance liquid chromatography analysis of this purified sphingolipid was performed to verify its purity. It was solubilised in chloroform: methanol (2:1 v/v). Samples (10 ng) were run on the column in a solvent system of linear gradient of isopropanol–hexane–water (55:40:5–55:38:7 v/v/v) at a flow rate of 0.5 ml/min for 100 min and the fraction was detected at 210 nm with Photo diode array detector. [HPLC Model used: LC-10AT, Shimadzu Corporation, Japan]. The column used was Iatrobead 6RSP 8010, 4.6 Id X 250 mm, Iatron laboratories, Inc.

MALDI-TOF analysis of PSL

Matrix-assisted laser desorption/ionisation time-of-flight is useful for structural investigation of lipids. The sample is dispersed in a large excess of matrix material, which will strongly absorb the incident light. A high-voltage tube accelerates the ions formed where they separate according to mass that is detected and recorded by a high-speed recording device. MALDI-TOF analysis was done on the placental purified sphingolipid (PSL) compound using Kratos PC Kompact instrument and Kratos standard software for data handling. The sample (1.0 mg) was dissolved in 100 μl of HPLC grade chloroform. The sample 0.2 μl (2 μg) was then mixed with 1 μl of the original matrix solution and spotted. The sample was charged with nitrogen laser with defined wavelength of 337 nm, acceleration voltage was to 20 kV. The ions were registered in a delayed reflector mode with 150 s delay time.

Fatty-acid analysis of PSL

The fatty acids in PSL were qualitatively and quantitatively analyzed by the method of Wollenweber et al., 1984. Briefly, 1 mg PSL was treated with anhydrous 2 N methanolic HCl and heated at 85°C for 16 h. The hydrolysate was concentrated using a N_2 stream and an equal volume of halfsaturated NaCl was added. The resulting methyl esters of fatty acids were extracted with distilled chloroform and finally subjected to GLC and GLC-MS. Fatty acids were determined as methyl ester derivatives by GLC comparing with those of authentic standards and also by the analysis of electron impact (EI) mass spectrometry.

Preparation of PSL for cell culture

As sphingolipids/ceramides are not soluble in aqueous medium and are usually emulsified with a protein (like a bovine serum albumin) to study their biological response (Zhang et al., 1990), PSL was first dissolved in chloroform/methanol (2:1 v/v) to take appropriate amounts in sterile experimental vials. After complete removal of the solvent, medium (DMEM containing 2% heat-inactivated FBS) was added, and then subjected to ultrasonication for uniform dispersion suitable for sphingolipid uptake by cells in culture. These were then used to study the effect of PSL by adding to the culture removing the spent medium and replaced by fresh medium. The viability of these cells was determined by the MTT [3-(4, 5-dimethyl-thiazol-2-yl)-2, 5-diphenyltetrazolium bromide] assay and trypan blue dye exclusion method (Mallick et al., 2002).

DOPA staining

Melanocyte cell-specific DOPA staining was performed on melanocytes according to the standard procedure of cell staining (Gilher et al., 1995). As stated earlier, human melanocytes cultured and maintained in MCDB-153 medium was trypsinised and seeded identically as for studying cellular morphology with a density of 1×10^3 cells/well of six-well TC-plates. After stipulated time of incubation with the desired stimulants, the media were aspirated off. The cells were fixed in 0.2 M cacodylate buffer containing 1% formalin for 2 h at 4°C. Following fixing in formalin containing buffer, the buffer was aspirated off and cells were washed to remove any formalin. The cells were finally incubated in 0.2 M cacodylate buffer, pH 7.2, containing 1% L-DOPA for 3–4 h depending upon the intensity of the staining required. The DOPA-stained cells were finally photographed.

Immunofluorescence staining

Immunofluorescence staining was carried out as described by Price et al., 1998. Human melanocytes were grown for 24 h on glass cover slips (2×10^4 cells/well) in a six-well plate and treated for stipulated time with or without 10 μg/ml of PSL. Cells were then rinsed briefly in 1× PBS fixed at room temperature for 20 min with 3% paraformaldehyde and permeabilised with pre-cold 100% methanol at −20°C for 5 min followed by blocking with 10% BSA in PBS for 30 min at room temperature. Cells were then incubated with primary antibody, anti-Tyrosinase (H-109) (1:100 dilution) (Santa Cruz Biotechnology, Inc.) for 2 h at room temperature. After washing with PBS three times, the cells were then incubated with secondary antibody, fluorescein-conjugated goat anti-rabbit antibody (1:50 dilution) (no. Sc-2012) (Santa Cruz Biotechnology, Inc.) for 1 h at 4°C. Then cells were washed in PBS and for DAPI staining, cells were simultaneously fixed and permeabilised using 2% paraformaldehyde and stained with 1 μg/ml of DAPI for 10 min at room temperature. The cells were viewed and photographed using inverted fluorescence microscope (Model: OLYMPUS 1×70; Olympus Optical Co. Ltd., Shibuya-ku, Tokyo, Japan).

Western blot analysis

Western blot analysis was performed to determine protein expression levels as previously described (Saha et al., 2006a,b). Briefly, 25 μg of total protein from each cell extract was electrophoresed in reducing SDS–(10%) PAGE and blotted on Polyvinylidene Fluoride (PVDF) membranes (Immobilon-P, Millipore Corporation, Bedford, MA, USA) using a Transblot system (Transblot SD: Semidry transfer cell; Bio-Rad Laboratories, Inc., Hercules, CA, USA). The membranes were then probed with primary antibodies overnight at 4°C and then incubated with horseradish peroxidase conjugated secondary antibody and signals were visualised with enhanced chemiluminescence (Cell Signaling Technology, Inc.). Loading control was assessed using antibodies to p38 MAP Kinase, CREB, MKK3, MKK6, MAPKAP kinase-2, and β-Actin. Membranes were processed for densitometric analysis using an imaging densitometer (Model: Image Scanner; Amersham Pharmacia Biotech, Buckinghamsire, UK) and a Software (Image Master Total lab version 1.11, from Phoretix, Newcastle upon Tyne, UK).

p38 MAPK assay

The activity of p38 MAP Kinase was analysed using a commercially available kit (p38 MAP Kinase assay Kit; Cell Signaling Technology). p38 MAP Kinase activity was analysed by a specific immunoprecipitation with antiphospho-specific p38 MAP Kinase antibody (Thr180/Tyr182) followed by an in vitro kinase assay of its substrate, ATF-2, according to the manufacturer's instruction as described previously (Singh et al., 2005). The samples were separated by a 10% SDS–PAGE, transferred to membranes and blotted with anti-phospho-specific ATF-2 antibody.

MAPKAP Kinase2 assay

The activity of MAPKAP Kinase2 was analysed using MAPKAP kinase2 assay kit (MAPKAP Kinase2 Immunoprecipitation Kinase

Assay Kit; non-radioactive; Upstate, Lake Placid, NY, USA) by a specific immunoprecipitation with anti MAPKAP Kinase2 antibody followed by an in vitro kinase assay of its substrate, Hsp27, according to the manufacturer's instruction. Briefly, 1 mg of cell lysates was incubated with 10 μl of resuspended anti MAPKAP Kinase2-agarose conjugate at 4°C for 1.5 h to immunoprecipitate MAPKAP Kinase2. The antibody/agarose/enzyme immunocomplex was washed with 100 μl ice-cold lysis buffer and subsequently with kinase buffer and then analysed for kinase activity. Immunoprecipitated MAPKAP Kinase2 was then incubated with 10 μl (0.5 μg) of recombinant Hsp27 in 50 μl of kinase buffer containing 100 μM ATP for 45 min at 30°C with vigorous shaking. The samples were then subjected to SDS–PAGE followed by immunoblotting with the phosphor-Hsp-27 antibody and a secondary antibody for enhanced chemiluminiscence.

Reporter and expression vectors

The expression vectors pMI (2135/+136), pMT2.2 (2236/+59) and pCMVβGal were gifted by Dr Robert Ballotti, Institut National de la Sante' et de la Researche Me' dicale, France. The plasmid pMI contains a 2.1-kb fragment of microphthalmia promoter upstream of the luciferase coding sequence in pGL2 basic vector. The plasmid pMT2.2 contains a 2.2-kb fragment of mouse tyrosinase promoter upstream of the luciferase coding sequence in pGL2 basic vector. The expression vector pRSV-Flag-MKK3 (Ala) and pcDNA3-Flag-MKK6 (K82A), encoding DN MKK3 and catalytically dead DN MKK6 respectively, were generous gift from Dr Roger Davis, University of Massachusetts, Worcester, MA, USA. pRSV-Flag-MKK3 (Ala) and pCDNA3-Flag-MKK6 (K82A) were constructed by replacing Ser-189 and Thr-193 with Ala and Lys-82 with Ala respectively (Raingeaud et al., 1996). The empty vector pcDNA3.1 (Invitrogen Life Technologies, Carlsbad, CA, USA) was used as a negative control.

Transfection and Reporter Assays

B16F10 melanoma cells were seeded in 24-well plate and after 24 h the cells were transiently transfected with 0.25 μg of the test plasmid (pMI, and pMT2.2) and 0.05 μg of pCMVβGal to control the variability in transfection efficiency, using Lipofectamine 2000. Twenty-four hours after transfection, cells were incubated with PSL for indicated times. Then the cells were washed with PBS and lysed using Reporter Lysis Buffer (Promega, Madison, WI, USA) and assayed for luciferase and β-Galactosidase activities using Luciferase Assay System and β-Galactosidase Enzyme Assay System respectively (Promega).

In experiments with DN MKK3 and DN MKK6, B16F10 cells were stably transfected with 3 μg of DN MKK3 and 3 μg of pcDNA3.1 or 3 μg of DN MKK6 and 3 μg of pcDNA3.1 or 3 μg of DN MKK3 and 3 μg of DN MKK6 or 6 μg of empty vector pcDNA3.1, all in the presence of 0.5 μg of pcDNA3.1/NT-GFP (Invitrogen Life Technologies) as a control to measure transfection efficiency, using Lipofectamine 2000 (Invitrogen Life Technologies). At 24 h after transfection, the transfected cells were selected with 1600 μg/ml G418. Then 1×10^6 stably transfected cells were plated per well in six-well plates and treated with 10 μg/ml of PSL for 1 h. The cells were then lysed and western blot analysis or p38 MAPK activity was measured.

Preparation of PSL for topical application on C57BL/6J mice skin

PSL was dissolved in 60% alcohol that facilitates penetration through skin. A working concentration of 10 μg/ml was prepared in 0.2 ml of total volume, which was applied per cm^2 each time with repeat of three times in a single application.

Topical application of the PSL on telogenic C57BL/6J mouse skin

Five mice were included in an experimental set. Body surface area of about 4 cm^2 on both sides was clipped to remove gray body coat hair to have the telogenic pinkish skin exposed, alcoholic extract was applied to the skin surface drop wise (0.2 ml/cm^2) with gentle rubbing (using the finger tips). On the opposite side of the same mouse, equivalent amount of 60% aqueous alcohol vehicle was applied identically. The process was repeated three times in a single application and each time was followed by irradiation with IR exposure (IR lamp, Infraphil, 230 V/150 W; Philips, Mumbai, India) from a distance of approximately 45 cm for 5 min. The whole process was carried out twice a day for a period of 45 days without any interruption in application programme. Changes in skin colour and associated hair growth were monitored on a regular basis.

Histological examination of C57BL/6J mice skin specimen

After local anaesthesia with lignocaine hydrochloride, skin specimens were dissected out by incisional biopsy (4–6 mm and full depth including subcutaneous tissue) from both the PSL and vehicle-treated sites. Skin samples were fixed in 10% neutral-buffered formalin and embedded in paraffin and then cut into 5 μm thick sections in a microtome. These were then stained by Masson–Fontana silver staining technique (Bancroft and Stevens, 1982) for melanin. Paraffin embedded tissue sections were also used for immunohistochemistry studies.

Masson–Fontana silver staining for melanin

Formalin fixed, paraffinised sections were deparaffinised in xylene and then hydrated. The sections were then treated with ammoniacal silver nitrate solution for 1 h at 63°C and then toned with 0.1% Gold Chloride for 10 min, washed with distilled water and subsequently treated with 5% sodium thiosulphate for 5 min and washed with distilled water. The sections were counterstained with 1% neutral red for 5 min. After washing in distilled water, the sections were dehydrated in 95% alcohol, absolute alcohol and cleared in xylene, and finally mounted in crystal mounting medium and observed under optical microscope (Model: OLYMPUS 1 × 70).

Immunohistochemistry

The expression of Mitf was viewed in skin tissue sections by indirect immunofluorescence using standard IHC techniques (Passeron et al., 2007). After deparaffinisation in xylene, skin samples were processed with ethanol and then treated with methanol at −20°C for 10 min. Subsequently it was incubated with 10 mM sodium citrate buffer (pH 6.0) at 95°C for 5 min for antigen retrieval and then immersed in blocking solution (10% goat serum containing 2% BSA) for 1 h at room temperature. The skin specimens were then incubated with primary antibody, rabbit antibody (1:10, diluted in 2% BSA) overnight at 4°C. This was washed in PBS three times 10 min each followed by incubation with second antibody, fluorescein isothiocyanate (FITC)-conjugated goat anti rabbit IgG (1:100, diluted in blocking serum) for 1 h at 37°C. Finally, the sections were washed three times with PBS for 15 min at each time and mounted in crystal mounting medium and observed under inverted fluorescence microscope (Model: OLYMPUS 1 × 70).

Statistics

Differences between results were assessed for significance using the Student's *t* test.

Acknowledgements

We are grateful to Prof. Colin R. Goding for his valuable advice, helpful discussion and critical editorial review of this manuscript. We thank Dr Robert Ballotti, National de la Santé et de la Researche Médicale, France, for providing expression vectors pMI (−2135/+136), pMImCRE, pMT2.2 (−2236/+59) and pCMV/βGal and Dr Roger Davis, Howard Hughes Medical Institute, Univ. of Mass. Medical School, Worcester, MA for the generous gift of the expression vectors pRSV-Flag-MKK3 (Ala) and pCDNA3-Flag-MKK6 (K82A). We also thank Dr Aurobindo Chowdhury of IICT, Hyderabad, India for helping MALDI-TOF analysis and our Director, Prof. Siddhartha Roy for his patronisation and keen interest in this work. Financial assistance from the CSIR (Council for Scientific and Industrial Research), and the DBT (Department of Biotechnology), New Delhi are thankfully acknowledged.

References

Bancroft, J.D., and Stevens, A. (1982). Theory and Practice of Histlogical Techniques (New York: Churchill Livingston).

Bhadra, R., Pal, P., Roy, R., and Dutta, A.K. (1994). Process for the preparation of an extract from human placenta containing glycosphingolipids and endothelin-like constituent peptides useful for the treatment of vitiligo. Indian patent appl. No. 1228/Del/94.

Bhadra, R., Pal, P., Roy, R., and Dutta, A.K. (1997). Process for the preparation of an extract from human placenta containing glycosphingolipids and endothelin-like constituent peptides useful for the treatment of vitiligo. US patent no. 5690966 Nov.25.

Bhadra, R., Pal, P., Roy, R., and Dutta, A.K. (1998). Process for the preparation of an extract from human placenta containing glycosphingolipids and endothelin-like constituent peptides useful for the treatment of vitiligo. European Union patent no. EP0839535.Dec6.

Carreira, S., Goodall, J., Denat, L., Rodriguez, M., Nuciforo, P., Hoek, K.S., Testori, A., Larue, L., and Goding, C.R. (2006). Mitf regulation of Dia1 controls melanoma proliferation and invasiveness. Genes Dev. *20*, 3426–3439.

Cui, J., Shen, L., and Wang, G. (1991). Role of hair follicles in the repigmentation of vitiligo. J. Invest. Dermatol. *97*, 410–416.

Deak, M., Clifton, A.D., Lucocq, J.M., and Alessi, D.R. (1998). Mitogen- and stress-activated protein kinase-1 (MSK1) is directly activated by MAPK and SAPK2/p38, and may mediate activation of CREB. EMBO J. *17*, 4426–4441.

Eisinger, M., and Marko, O. (1982). Selective proliferation of normal human melanocytes in vitro in the presence of phorbol ester and cholera toxin. Proc. Natl. Acad. Sci. U.S.A. *79*, 2018–2022.

Falabella, R., and Barona, M.I. (2009). Update on skin repigmentation therapies in vitiligo. Pigment Cell Melanoma Res. *22*, 42–65.

Fitzpatrick, T.B., Szabo, S., and Wick, M.M. (1983). Biochemistry and physiology of melanin Pigmentation. In Biochemistry and Physiology of the Skin, L.A. Goldsmith, ed. (New York: Oxford University Press), pp. 687–712.

Fuchs, E., Merrill, B.J., Jamora, C., and DasGupta, R. (2001). At the roots of a never-ending cycle. Dev Cell. *1*, 13–25.

Gilher, A., Gershoni-Baruch, R., Margolis, A., Benderly, A., and Brandes, J.M. (1995). Dopa reactions of fetal melanocytes before and after transplantation on to nude mice. Br. J. Dermatol. *133*, 884–889.

Higuchi, K., Kawashima, M., Ichikawa, Y., and Imokawa, G. (2003). Sphingosylphosphoryl-choline is a melanogenic stimulator for human melanocytes. Pigment Cell Res. *16*, 670–678.

Hodgkinson, C.A., Moore, K.J., Nakayama, A., Steingrimsson, E., Copeland, N.G., Jenkins, N.A., and Arnheiter, H. (1993). Mutations at the mouse microphthalmia locus are associated with defects in a gene encoding a novel basic-helix-loop-helixzipper protein. Cell *74*, 395–404.

Hughes, M.J., Lingrel, J.B., Krakowsky, J.M., and Anderson, K.P. (1993). A helix–loop–helix transcription factor-like gene is located at the *mi* locus. J. Biol. Chem. *268*, 20687–20690.

Kaidbey, K.H., Agin, P.P., Sayre, R.M., and Kligman, A.M. (1979). hotoprotection by melanin—a comparison of black and Caucasian skin. J. Am. Acad. Dermatol. *1*, 249–260.

King, R., Weilbaecher, K.N., McGill, G., Cooley, E., Mihm, M., and Fisher, D.E. (1999). Microophthalmia transcription factor: sensitive and specific melanocyte marker for melanoma diagnosis. Am. J. Pathol. *155*, 731–738.

Kollias, N., Sayer, R.M., Zeise, L., and Chedekel, M.R. (1991). Photoprotection by melanin. J. Photochem. Photobiol. B. Biol. *9*, 135–160.

Mallick, S., Mandal, S.K., and Bhadra, R. (2002). Human placental lipid induces mitogenesis and melanogenesis in B16F10 melanoma cells. J. Biosc. *27*, 243–249.

Mallick, S., Singh, S.K., Sarkar, C., Saha, B., and Bhadra, R. (2005). Human placental lipid induces melanogenesis by increasing the expression of tyrosinase and its related proteins in vitro. Pigment Cell Res. *18*, 25–33.

McGill, G.G., Horstmann, M., Widlund, H.R. et al. (2002). Bcl2 regulation by the melanocyte master regulator Mitf modulates lineage survival and melanoma cell viability. Cell *109*, 707–718.

Medrano, E.E., and Nordlund, J.J. (1990). Successful culture of adult human melanocytes obtained from normal and vitiligo donors. J. Invest. Dermatol. *95*, 441–445.

Nishimura, E.K., Jordan, S.A., Oshima, H., Yoshida, H., Osawa, M., Moriyama, M., Jackson, I.J., Barrandon, Y., Miyachi, Y., and Nishikawa, S. (2002). Dominant role of the niche in melanocyte stem-cell fate determination. Nature *416*, 854–860.

Nishimura, E.K., Granter, S.R., and Fisher, D.E. (2005). Mechanisms of hair graying: incomplete melanocyte stem cell maintenance in the niche. Science, *307*, 720–724.

Ortonne, J.P., and Prota, G. (1993). Hair melanins and hair colour: ultrastructure and biochemical aspects. J. Invest. Dermatol. *101*, 82S–89S.

Osawa, M., Egawa, G., Mak, S.S., Moriyama, M., Freter, R., Yonetani, S., Beermann, F., and Nishikawa, S. (2005). Molecular characterization of melanocyte stem cells in their niche. Development *132*, 5589–5599.

Osborne J.C. Jr (1986). De-Lipidation of Plasma Lipoproteins. Methods in Enzymology Vol. 128 (New York: Academic Press Inc.), pp. 213–222.

Pal, P., Roy, R., Datta, P.K., Biswas, B., and Bhadra, R. (1995). ydroalcoholic human placenta extract skin pigmenting activity and gross chemical composition. Int. J. Dermatol. *34*, 61–66.

Pal, P., Mallick, S., Mandal, S.K., Das, M., Dutta, P.K., Datta, A.K., Bera, R., and Bhadra, R. (2002). A human placental extract: in vivo and in vitro assessments of its melanocyte growth and pigment inducing activities. Int. J. Dermatol. *41*, 760–767.

Passeron, T., Coelho, S.G., Miyamura, Y., Takahashi, K., and Hearing, V.J. (2007). Immunohistochemistry and in situ hybridization in the study of human skin melanocytes. Exp. Dermatol. *16*, 162–170.

Price, E.R., Horstmann, M.A., Wells, A.G., Weilbaecher, K.N., Takemoto, C.M., Landis, M.W., and Fisher, D.E. (1998). α-Melanocyte-stimulating hormone signaling regulates expression of microphthalmia, a gene deficient in Waardenburg syndrome. J. Biol. Chem. *273*, 33042–33047.

Raingeaud, J., Whitmarsh, A.J., Barrett, T., Derijard, B., and Davis, R.J. (1996). MKK3- and MKK6-regulated gene expression is

mediated by the p38 mitogen-activated protein kinase signal transduction pathway. Mol. Cell. Biol. *16*, 1247–1255.

Rouse, J., Cohen, P., Trigon, S., Morange, M., Alonso-Llamazares, A., Zamanillo, D., Hunt, T., and Nebreda, A.R. (1994). A novel kinase cascade triggered by stress and heat shock that stimulates MAPKAP kinase-2 and phosphorylation of the small heat shock proteins. Cell *78*, 1027–1037.

Saha, B., Singh, S.K., Sarkar, C., Mallick, S., Bera, R., and Bhadra, R. (2006a). Transcriptional activation of Tyrosinase gene by Human placental sphingolipid. Glycoconj. J. *23*, 261–269.

Saha, B., Singh, S.K., Sarkar, C., Bera, R., Ratha, J., Tobin, D.J., and Bhadra, R. (2006b). Activation of the Mitf promoter by lipid-stimulated activation of p38-stress signalling to CREB. Pigment Cell Res., *19*, 595–605.

Siddiqui, K.A.I., Sett, S., Mishra, S., Datta, P.K., Pal, P., Mallick, S., Mandal, S.K., and Bhadra, R. (1998). A process for the preparation of a ceramide from placental extract useful as an inducer of melanin in eukaryotic system. (filed in India, application no. 1675/Del/98).

Silva-Vargas, V., Lo Celso, C., Giangreco, A., Ofstad, T., Prowse, D.M., Braun, K.M., and Watt, F.M. (2005). Beta-catenin and Hedgehog signal strength can specify number and location of hair follicles in adult epidermis without recruitment of bulge stem cells. Dev Cell *9*, 121–131.

Singh, S.K., Sarkar, C., Mallick, S., Saha, B., Bera, R., and Bhadra, R. (2005). Human placental lipid induces melanogenesis through p38 MAPK In B16F10 mouse melanoma. Pigment Cell Res. *18*, 113–121.

Slominski, A., and Paus, R. (1993). Melanogenesis is coupled to murine anagen: toward new concepts for the role of melanocytes and the regulation of melanogenesis in hair growth. J. Invest. Dermatol. *10*, 90S–97S.

Spritz, R.A. (2007). The genetics of generalized vitiligo and associated autoimmune diseases. Pigment Cell Res. *20*, 271–278.

Stokoe, D., Caudwell, B., Cohen, P.T., and Cohen, P. (1993). The substrate specificity and structure of mitogen-activated protein (MAP) kinase-activated protein kinase-2. Biochem. J. *296*, 843–849.

Swart, J.M., Bergeron, D.M., and Chiles, T.C. (2000). Identification of a membrane Ig-induced p38 mitogen-activated protein kinase module that regulates campresponse element binding protein phosphorylaation and transcriptional activation in CH31 B cell lymphomas. J. Immunol. *164*, 2311–2319.

Tachibana, M. (2000). MITF: a stream flowing for pigment cells. Pigment Cell Res. *13*, 230–240.

Takeda, K., Yasumoto, K., Takada, R., Takada, S., Watanabe, K., Udono, T., Saito, H., Takahashi, K., and Shibahara, S. (2000). Induction of melanocyte-specific microphthalmia-associated transcription factor by Wnt-3a. J. Biol. Chem. *275*, 14013–14016.

Tan, Y., Rouse, J., Zhang, A., Cariati, S., Cohen, P., and Comb, M.J. (1996). FGF and stress regulate CREB and ATF-1 via a pathway involving p38 MAP kinase and MAPKAP kinase-2. EMBO J. *15*, 4629–4642.

Vance, K.W., and Goding, C.R. (2004). The transcription network regulating melanocyte development and melanoma. Pigment Cell Res. *17*, 318–325.

Westerhof, W., and d'Ischia, M. (2007). Vitiligo puzzle: the pieces fall in place. Pigment Cell Res. *20*, 345–359.

Wollenweber, H.W., Seydel, U., Lindner, B., Luderitz, O., and Rietschel, E.T. (1984). Nature and location of amide-bound (R)-3-acyloxyacyl groups in lipid A of lipopolysaccharides from various gramnegative bacteria. Eur. J. Biochem. *145*, 265–272.

Yoshida, H., Kunisada, T., Kusakabe, M., Nishikawa, S., and Nishikawa, S.I. (1996). Distinct stages of melanocyte differentiation revealed by analysis of nonuniform pigmentation patterns. Development. *122*, 1207–1214.

Zhang, H., Desai, N.N., Murphey, J.M., and Spiegel, S. (1990). Sphingosine stimulates cellular proliferation via a protein kinase C-independent pathway. J. Biol. Chem. *265*, 21309–21316.